ASTRONOMICAL JOURNAL, 119:2535–2539, 2000 June

A CLOSE-SEPARATION DOUBLE QUASAR LENSED BY A GAS-RICH GALAXY[1]

MICHAEL D. GREGG,[2,3] LUTZ WISOTZKI,[4,5] ROBERT H. BECKER,[2,3] JOSÉ MAZA,[6] PAUL L. SCHECHTER,[5,7] RICHARD L. WHITE,[8] MICHAEL S. BROTHERTON,[9] AND JOSHUA N. WINN[5,7]

Received 2000 February 15; accepted 2000 March 9

ABSTRACT

In the course of a Cycle 8 snapshot imaging survey with the Space Telescope Imaging Spectrograph (STIS), we have discovered that the $z = 1.565$ quasar HE 0512−3329 is a double with image separation 0.″644, differing in brightness by only 0.4 mag. This system is almost certainly gravitationally lensed. Although separate spectra for the two images have not yet been obtained, the possibility that either component is a Galactic star is ruled out by a high signal-to-noise composite ground-based spectrum and separate photometry for the two components: the spectrum shows no trace of any zero-redshift stellar absorption features belonging to a star with the temperature indicated by the broadband photometry. The optical spectrum shows strong absorption features of Mg II, Mg I, Fe II, Fe I, and Ca I, all at an identical intervening redshift of $z = 0.9313$, probably due to the lensing object. The strength of Mg II and the presence of the other low-ionization absorption features is strong evidence for a damped Lyα system, likely the disk of a spiral galaxy. Point-spread function fitting to remove the two quasar components from the STIS image leads to a tentative detection of a third object, which may be the nucleus of the lensing galaxy. The brighter component is significantly redder than the fainter, due to either differential extinction or microlensing.

Key words: gravitational lensing — quasars: individual (HE 0512−3329)

1. INTRODUCTION

The study of gravitationally lensed quasars has become a powerful tool for addressing a number of astrophysical questions. In particular, concentrating on studying the lensing objects themselves provides a sample of distant galaxies selected by mass rather than by light (Kochanek et al. 2000). Because the component separations scale with the square root of the mass of the lens, sampling the low end of the lens mass function becomes difficult from the ground, particularly in the optical/IR, for separations $\lesssim 1''$. This observational bias leads to a preponderance of massive spheroidal galaxies in the present sample of lenses and at least partly accounts for the relative lack of known close-separation lenses, which are predicted to exist by theoretical models of the lensing phenomenon (e.g., Maoz & Rix 1993; Rix et al. 1994; Jain et al. 1999). There are currently only seven systems with separations $\leq 0.''9$ out of 43 confirmed lensed quasars listed in the CASTLE Survey.[10]

We are now well into a Cycle 8 snapshot survey of up to 300 targets, aimed specifically at finding close-separation lensed quasars using the imaging capabilities of the Space Telescope Imaging Spectrograph (STIS; Kimble et al. 1997; Woodgate et al. 1998) on board *Hubble Space Telescope*. The probability that a quasar is lensed increases with redshift and apparent magnitude (Turner, Ostriker, & Gott 1984); the snapshot survey targets bright, high-redshift quasars selected using estimates for the probability of lensing by Kochanek (1998, private communication). The results of the full snapshot survey will appear in time (Gregg et al. 2000); here we report the discovery of a close-separation gravitationally lensed quasar from among the first 80 snapshot targets.

2. OBSERVATIONS

2.1. *Discovery*

The quasar HE 0512−3329 was originally identified in the Hamburg/ESO survey for bright QSOs (Wisotzki et al. 1996). With $B = 17.0$ and $z = 1.569$ (Reimers, Köhler, & Wisotzki 1996), HE 0512−3329 had an a priori probability of ∼1.3% of being lensed, fairly typical for the targets in our snapshot survey. The STIS snapshot sequence, obtained on 1999 August 26, consists of 3 × 40 s CR-split exposures in the clear 50CCD (CL) aperture and one additional 80 s CR-split exposure in the long-pass F28 × 50LP (LP) filter. The effective wavelength and full width half maximum of the CL band are 6167.6 Å and 4410 Å and for the LP band are 7333 Å and 2721 Å. The STIS images reveal two point sources with a separation of 0.″644. The difference in brightness between the two components A and B is $\Delta CL = 0.35$ and $\Delta LP = 0.49$; this small difference is characteristic of the more highly magnified lensed systems, which our selection technique is designed to favor.

The lensing hypothesis was strengthened by examining the discovery spectrum of HE 0512−3329, which shows a rather typical quasar energy distribution having emission lines of C IV 1549 and C III] 1909 (see Fig. 1 of Reimers et al. 1996). If one of the two components were a garden variety Galactic star, the strongest stellar absorption lines would be easily identifiable (see § 2.3). A binary quasar is a possible alternative explanation (Kochanek, Falco, & Muñoz

[1] Based on observations with the NASA/ESA *Hubble Space Telescope*, obtained at the Space Telescope Science Institute, which is operated by the Association of Universities for Research in Astronomy (AURA), Inc., under NASA contract NAS 5-26555.

[2] Department of Physics, University of California at Davis, Davis, CA 95616; gregg,bob@igpp.llnl.gov.

[3] Institute for Geophysics and Planetary Physics, Lawrence Livermore National Laboratory.

[4] Hamburger Sternwarte, Germany; lwisotzki@hs.uni-hamburg.de.

[5] Massachusetts Institute of Technology; schech@achernar.mit.edu, jnwinn@mit.edu.

[6] Universidad de Chile; jose@das.uchile.cl.

[7] Visiting Astronomer, Cerro Tololo Inter-American Observatory, National Optical Astronomy Observatories (NOAO).

[8] Space Telescope Science Institute; rlw@stsci.edu.

[9] Kitt Peak National Observatory; mbrother@noao.edu.

[10] Available at http://cfa_www.harvard.edu/castles.

1999b), however, the discovery spectrum exhibits a strong absorption feature consistent with Mg II at an intervening redshift of 0.93 and a few weaker absorption lines of Fe II at the same redshift. These low-ionization absorption features suggested that the duplicity is due to a lensing object at this redshift.

2.2. *Follow-up Spectroscopy at Keck Observatory*

In early 2000 January, we obtained a 9 Å resolution spectrum of HE 0512−3329 using the Low Resolution Imaging Spectrograph (LRIS, Oke et al. 1995) at Keck Observatory. The slit was oriented at the position angle of the two quasar images on the sky, 17°. The seeing was 1″, insufficient to resolve the components. From this 300 s exposure (Fig. 1), we obtain a redshift of 1.565 ± 0.001 based on Gaussian fits to the C IV and C III] emission peaks. The S/N of this new spectrum is 50 to 100 over most of its wavelength range and confirms the presence of the strong intervening absorption, clearly resolving the Mg II 2796.4, 2803.5 doublet and detecting the associated Mg I 2853 line. Also seen is a rich absorption system of Fe II 2260.8, 2344.2, 2374.5, 2382.8, 2586.7, and 2600.2, and Ca I 4227.9 belonging to the same intervening system; Ca II 3933 and 3969 fall in the atmospheric A band. The mean of the absorption redshifts is $z = 0.9313 \pm 0.0005$. The profile of the Mg II emission line is asymmetric, which can be attributed to absorption by Fe I 3721.0 or intervening Mg II local to the quasar. There is another weak intervening Mg II absorption feature at $z = 1.1346$.

Component B is 70% the brightness of A. The lack of any discernible stellar absorption features in the Keck spectrum (Fig. 1) argues strongly against component B being a foreground star. The rms noise in the spectrum is at the level of 0.15 Å equivalent width. The strongest features in late-type stars have equivalent widths of a few angstroms and would be detected easily in the Keck spectrum; for comparison, the equivalent width of the intervening Mg I 2853 Å feature is 1.4 Å. The only possible stellar contaminant is a completely featureless O-type subdwarf or white dwarf and such stars are extremely rare. If this were the case, however, the spectrum of HE 0512−3329 would be much bluer, unless either the QSO or the putative star has a large amount of intrinsic reddening.

2.3. *Photometry*

We have done point-spread function (PSF) fitting photometry on the STIS images using IRAF/DAOPHOT. From observations of an unlensed quasar in our program, we obtain aperture corrections of −0.222 and −0.303 for the CL and LP bands, to go from the fitted 3 pixel radius to 0.″5. To this we add an additional −0.1 mag to correct to the "true" magnitude in an infinite aperture, as is standard practice with WFPC2 (Holtzman et al. 1995). The resulting calibrated STIS "ST magnitudes" and errors are listed in Table 1.

The LP bandpass is completely contained within the CL. Because they are similar in shape, the LP flux can be scaled by the relative throughputs and subtracted from the CL, producing an effective "short-pass" measurement (Gregg & Minniti 1997; Gardner et al. 2000) extending from 5500 to 2000 Å, with effective wavelength of 4424 Å and FWHM of 2569 Å. The SP−LP difference provides some wide-band color information (Table 1).

In 1999 December, we obtained *VRI* photometry of HE 0512−3329 using the Mosaic II CCD imager at the Blanco 4 m telescope at Cerro Tololo Inter-American Observatory (CTIO).[11] Although the seeing was ∼0.″8–0.″9 and the two components are not cleanly resolved, PSF fitting using IRAF/DAOPHOT successfully separated them, yielding positions in excellent agreement with the *HST* images and photometry consistent with the STIS results. The separa-

[11] Cerro Tololo Inter-American Observatory, NOAO, is operated by AURA under cooperative agreement with the National Science Foundation.

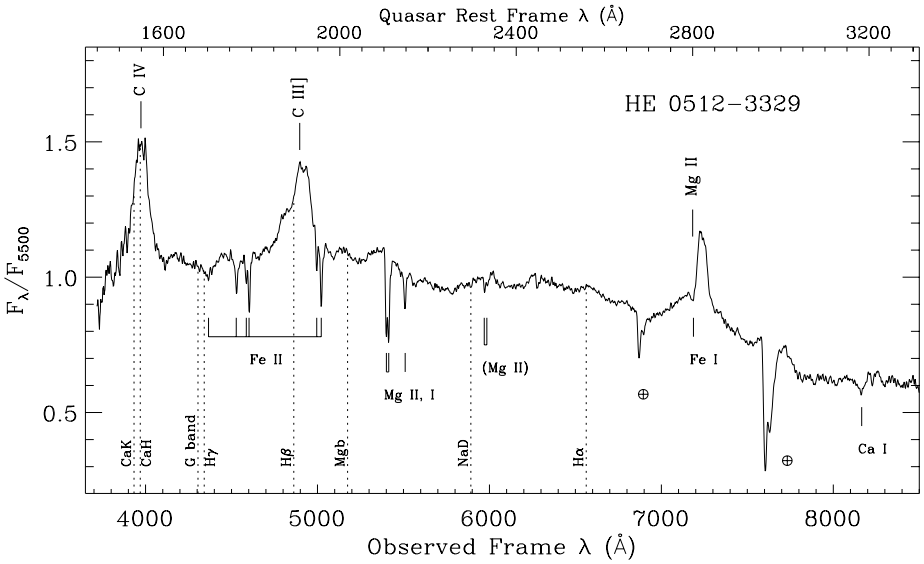

FIG. 1.—Keck LRIS 9 Å resolution spectrum of HE 0512−3329 obtained in 2000 January. The top abscissa scale is the rest frame of the quasar with a redshift of 1.565; prominent emission-line features are marked above the spectrum. Lines associated with the intervening system at $z = 0.9313$ are identified below the spectrum. The absorption lines are probably due to the lensing galaxy and are unresolved at the instrumental resolution. There is a second rather weak intervening Mg II 2800 absorption system at $z = 1.1346$ (in parentheses). The small difference in brightness of the two components and the lack of any visible stellar absorption features (*dotted lines*) in this high S/N composite spectrum argues strongly against component B being a foreground star.

TABLE 1

HE 0512−3329

Object	R.A.	Decl.	CL	LP	SP	*B*	*V*	*R*	*I*
A	05 14 10.7833	−33 26 22.504	17.94	18.53	19.47	18.36	17.68	17.22	16.86
B	05 14 10.7687	−33 26 23.121	18.28	19.03	19.46	18.35	18.03	17.66	17.34
B−A.....	−0.″183	0.″618	0.35	0.49	−0.01	−0.01	0.35	0.44	0.48
Errors.....	0.″003	0.″003	0.02	0.02	0.02	0.04	0.02	0.02	0.02

NOTE.—Units of right ascension are hours, minutes, and seconds, and units of declination are degrees, arcminutes, and arcseconds (J2000.0). Photometry is uncorrected for Galactic reddening. Errors are statistical only.

tions obtained in *V*, *R*, and *I* are 0.″654, 0.″646, and 0.″643, respectively, compared with 0.″644 obtained from the centroids of the components in the STIS CL images.

No photometric standards were taken at CTIO, so we have calibrated the CTIO photometry using zero points determined by convolving the Keck spectrophotometry with Cousins *VRI* passbands. This procedure is itself calibrated using a model for the spectrum of Vega (Kurucz 1992, private communication) for which we adopt $B = V = R = I = 0.0$. Slit losses limit the absolute accuracy, but, fortuitously, the spectroscopy was obtained when the position angle of HE 0512−3329 was only 23° from the parallactic angle. Because the effective slit width was somewhat greater than the atmospheric dispersion between the red and blue extremes of the spectrum (Filippenko 1982), the colors obtained from the composite spectrum are reasonably accurate and can be used to establish the relative zero points of the *VRI* photometry. Also, we have determined a zero-point transformation between the effective STIS SP bandpass and Johnson B using the mean quasar spectrum (Brotherton et al. 2000) from the FIRST Bright Quasar Survey (FBQS; White et al. 2000), redshifted to $z = 1.565$. The resulting colors of HE 0512−3329 are $B-V = 0.68$, $V-R = 0.46$, $V-I = 0.82$ for component A, and $B-V = 0.32$, $V-R = 0.37$, $V-I = 0.69$ for component B (Table 1). Schlegel, Finkbeiner, & Davis (1998) estimate a Galactic extinction of $A_B = 0.104$ for this line of sight; Burstein & Heiles (1982) give a much lower value of 0.010. The numbers in Table 1 have not been corrected for Galactic extinction.

The broadband colors of the two components clinch the case for HE 0512−3329 being a lensed quasar. By comparison with the 1996 Bruzual et al. stellar library,[12] the $B-V$ color of component B indicates a spectral type of F0, yet $V-R$ and $V-I$ are consistent with a much cooler object, about F9/G0. Our simulations show that any star in this spectral range with the relative brightness of component B would contribute easily detectable absorption features, at $\sim 10\ \sigma$ level or greater, to the composite spectrum at the indicated locations in Figure 1; Ca II H and K and the Balmer lines would be particularly conspicuous. The broadband colors of component B are, in fact, more consistent with a slightly reddened quasar than a star.

For future reference for monitoring variability of the lens components, we list in Table 2 the instrumental magnitude differences $m_i - m_A$ for nine field stars with $V \approx 16$ to 18 in the vicinity of HE 0512−3329. The astrometry has been derived from the digitized sky survey and has an offset of ΔR.A. = +0.″55 and Δdecl. = +0.″77 relative to the STIS images, but these positions are sufficient to unambiguously identify the comparison stars.

[12] Available at ftp://ftp.stsci.edu/cdbs/cdbs2/grid/bpgs.

TABLE 2

FIELD STAR DIFFERENCE PHOTOMETRY

Object	R.A.	Decl.	ΔV_i	ΔR_i	ΔI_i
Star 1−A.....	5 14 08.98	−33 27 08.1	−1.04	−1.14	−1.12
Star 2−A.....	5 14 11.62	−33 26 50.1	0.56	0.77	0.95
Star 3−A.....	5 14 14.83	−33 27 24.7	0.91	0.93	0.96
Star 4−A.....	5 14 18.74	−33 26 03.6	−0.38	−0.38	−0.32
Star 5−A.....	5 14 19.06	−33 26 13.6	1.33	0.99	0.72
Star 6−A.....	5 14 08.63	−33 24 26.9	−0.30	−0.17	−0.09
Star 7−A.....	5 14 08.51	−33 24 48.4	0.81	0.78	0.77
Star 8−A.....	5 13 57.75	−33 26 24.3	1.25	0.88	0.54
Star 9−A.....	5 14 05.42	−33 29 15.7	−0.58	−0.42	−0.29

NOTE.—Units of right ascension are hours, minutes, and seconds, and units of declination are degrees, arcminutes, and arcseconds (J2000.0). Numbers are instrumental magnitude differences $m_{star} - m_A$ in the Cousins system; no color terms have been applied.

3. THE NATURE OF THE LENSING OBJECT

The presence of the strong intervening Mg II absorption and the many associated low ionization lines are evidence that the lensing object contains a damped Lyα absorption (DLA) system (Boisse et al. 1998). A DLA system at a redshift <1 is most likely to be the hydrogen-rich disk of a spiral galaxy. Dust in the galaxy may produce differential reddening in the two components of HE 0512−3329.

3.1. *Possible Detection of a Third Object*

To explore for the lensing galaxy and possible additional quasar images, the STIS CL images were combined using the DRIZZLE package (Fruchter & Hook 1998) in IRAF/STSDAS. A sampling rate of 0.5 times the original image scale and a PIXFRAC value of 0.6 were used. The subpixel image shifts were determined using the IRAF task XREGISTER. The final combined CL image is shown in the left panel of Figure 2. The distance between centroids of the two images is 0.″644; at the probable lens redshift of 0.9313, this separation is only ~ 4 kpc, adopting $H_0 = 70$ km s^{-1} Mpc^{-1} and $q_0 = 0.5$. The mass associated with an Einstein ring of this scale is $\sim 3 \times 10^{10}\ M_\odot$.

The PSF removal was done using the SCLEAN task in IRAF/STSDAS. For the PSF itself, we used the theoretical STIS PSF from the TinyTim package and also the STIS PSF generated by the Hubble Deep Field South project (Gardner et al. 2000). They yield very similar results. The residual image is shown in the right-hand panel of Figure 2. There is an excess of counts just above and to the right of component A (white arrow in Fig. 2). The RMS in the background-subtracted image is approximately ± 1.3

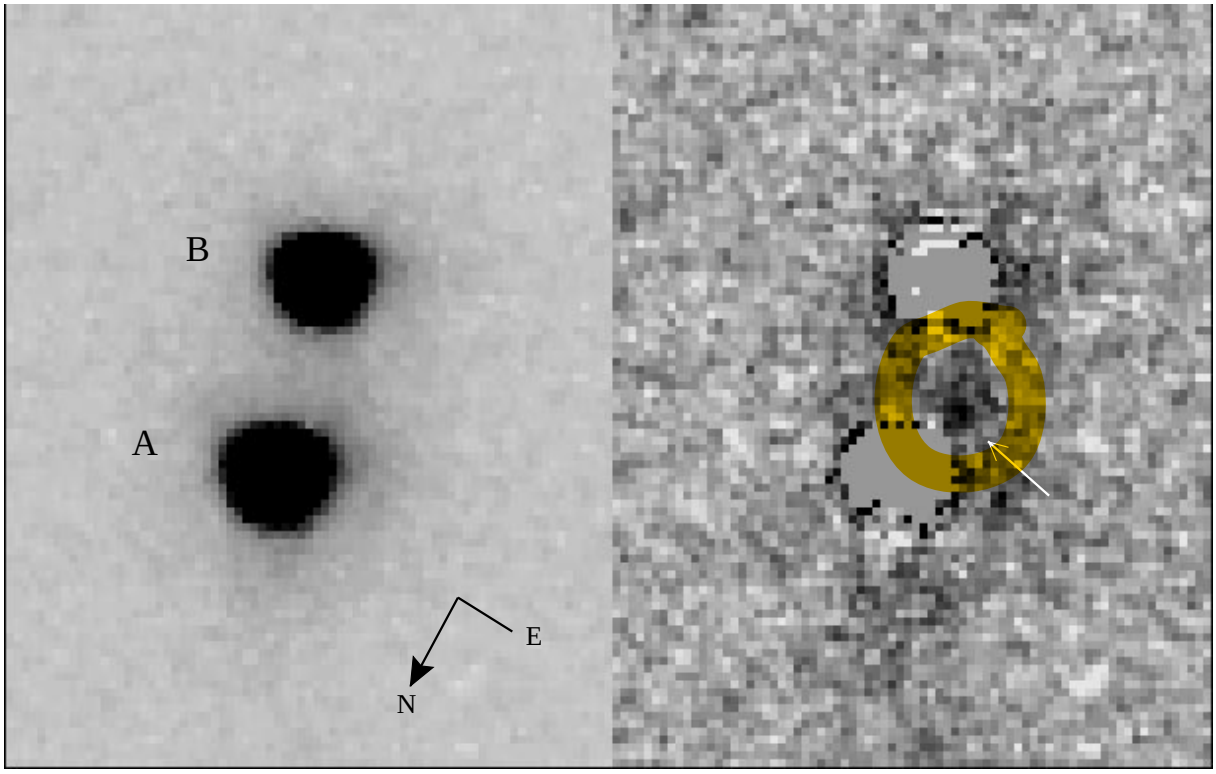

FIG. 2.—*Left*: STIS 50CCD (CL) image of HE 0512−3329. Component A is 0.35 mag brighter than B in this passband. The separation is 0.″644. The orientation is given by the compass points; the north arrow is 0.″25 long. *Right*: Residuals after PSF removal. The object immediately above and to the right of A (indicated by the white arrow) may be the nucleus of the lensing galaxy. There is also excess low surface brightness flux around each component.

counts while the peak in the excess region is 8.7. The total flux is ∼5.9 mag fainter than component A, giving it CL = 23.8. Its FWHM is roughly twice that of a point source, consistent with being nonstellar. We tentatively identify this object as the nucleus of the lensing galaxy. For our adopted cosmology, this object has $M_V \approx -19$, roughly the nucleus of a roughly L^* galaxy with a bulge-to-disk ratio of ∼3 and, for the above quoted Einstein ring mass, a M/L ratio of ∼20. At the intervening redshift of 0.9313, the two lines of sight to the quasar pass 1.6 (A) and 2.7 (B) kpc from the position of the third object.

There is excess light of lower surface brightness between the two quasar images and immediately below component A as well as to the right of component B in Figure 2. Although the third object is not detected with confidence in the LP image, the low surface brightness light distribution is qualitatively reproduced in the redder passband. No such excess light is seen when the same analysis is applied to an image of an unlensed quasar from our snapshot program. Deeper images are needed to confirm the reality of this low surface brightness fuzz and, if real, determine whether it is due to the lens, the host galaxy, or another object.

3.2. *Reddening Analysis*

The STIS and ground-based photometry are consistent in showing that component A is redder than B. Going from red to blue, the magnitude difference between the two images decreases, becoming equal within the errors in the concocted STIS SP and transformed B bands (Fig. 3). Observed in the ultraviolet, component B will be the brighter. This trend can be attributed to differential reddening, with extinction along the line of sight to component A being greater. Color differences between the quasar images can also be arise from microlensing by stars in the lensing galaxy, producing differential magnification of the quasar continuum (Wambsganss & Paczyński 1991) along the two lines of sight. This effect has been observed in at least one quasar, HE 1104−1805 (Wisotzki et al. 1993). The following reddening analysis is valid only if microlensing is negligible in HE 0512−3329.

To quantify the amount of differential reddening, we have fitted an extinction model to the photometry results, following the procedure of Falco et al. (1999). In this approach, it

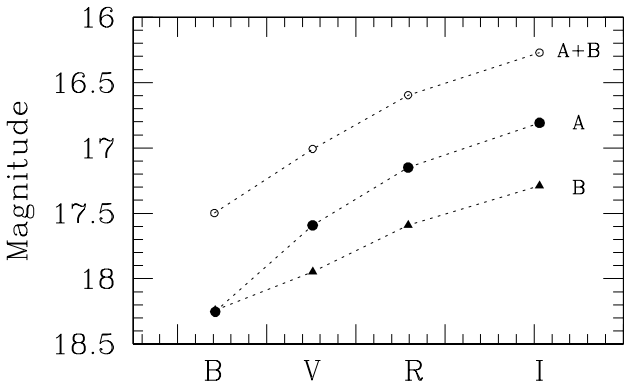

FIG. 3.—Trend of the broadband magnitudes of HE 0512−3329 for components A, B, and the composite A + B. The *VRI* photometry is from the ground-based CTIO imaging, while the *B* magnitudes are derived from the difference between the STIS CL and LP bands; both have been zero-pointed using the Keck spectrophotometry in Fig. 1 (see text for details). The brightness of the two images converges from red to blue. This can be attributed to differential extinction or microlensing, possibly both. These data have been corrected from Table 1 for Galactic absorption of $A_B = 0.104$

is assumed that the quasar is not variable, that the lensing magnification is not wavelength dependent, and that the extinction law does not vary with position in the lensing galaxy and is well approximated by a typical Galactic extinction curve with $R_V = E(B-V)/A_V = 3.1$. Correcting a sign error in equation (3) of Falco et al., we have

$$\chi^2 = \sum_{j=1}^{N_\lambda} \sum_{i=1}^{N_c} \times \frac{\{m_i(\lambda_j) - m_0(\lambda_j) + 2.5 \log (M_i) - E_i R[\lambda_j/(1+z)]\}^2}{\sigma_{ij}^2}, \quad (1)$$

where m_i are the observed magnitudes of each of the N_c components in the N_λ photometric bands with effective wavelength λ_j, m_0 is the unlensed magnitude of the quasar, M_i is magnification of each component, E_i is the extinction of each component, z is the redshift of the lens, and σ_{ij} are the photometric errors. The summations are over the four bandpasses, B, V, R, and I, and two components, A and B.

Relative magnifications and extinctions can be found by minimizing χ^2 while holding one magnification fixed at unity and one extinction at 0. As component B is bluer and fainter, we fix its parameters at these values. The extinction law has been parametrized using the equations of Cardelli, Clayton, & Mathis (1989). For this analysis, we first corrected the photometry listed in Table 1 for Galactic extinction of $A_B = 0.104$ from Schlegel et al. (1998).

The fit for the relative extinction results in the estimate of $A_V = 0.34$ for component A, in excess of the extinction at component B; the unextincted, wavelength-independent relative magnification of A is 2.45 times that of B. The χ^2 of this fit is 0.66. For comparison, a fit with both extinctions held to zero yields a relative magnification of 1.35, roughly consistent with the brightness difference between the two components in V or R. The χ^2 for this fit is 67, as might be expected given the varying magnitude difference between the two components as a function of wavelength, which renders an achromatic magnification model a poor explanation of the brightness variation with wavelength.

The separate extinctions to each component of HE 0512−3326 can be estimated by assuming that the unlensed quasar spectrum has typical colors. After correcting for Galactic reddening using the Schlegel et al. (1998) value, the difference in $B-V$ between the composite spectrum of HE 0512−3326 (Fig. 1) and the FBQS mean spectrum is 0.31. With $R_V = 3.1$, this is equivalent to $A_V = 0.97$. Knowing the V magnitudes and relative extinction, the separate extinctions can be computed as $A_V^A = 1.10$ and $A_V^B = 0.76$, excluding any gray component. Given the multitude of assumptions and the bootstrapping from the spectrophotometry, these numbers must be considered provisional, but they do suggest that the extinction to each component is comparable and that both lines of sight intercept the same or similar absorption systems. Spectroscopy of the two components separately would allow a detailed study of the extinction curve in the disk of the lensing galaxy and would also determine whether microlensing could be contributing to the pattern of color differences.

4. CONCLUSION

The presently available data leave little doubt that HE 0512−3329 is gravitationally lensed. The spectroscopic evidence strongly suggests that the lens is a spiral galaxy. Spatially resolved spectroscopy of the two images of HE 0512−3329 is needed to confirm its nature; however, the presence of strong low-ionization lines in the composite spectrum indicates that at least one of the lines of sight is sure to pass through a damped Lyα system in the disk of the lens. Ultraviolet spectroscopy of the A and B components can further be used to derive the extinction curve in the disk of the lens as well as abundances of heavy elements. This lensed quasar has been found among the first 80 targets of an *HST* Cycle 8 snapshot program designed to search for such small separation systems. The program was renewed for up to 300 additional snapshots in Cycle 9. If close-separation targets are found with this frequency for the duration of the survey, the lensing statistics for small separation systems will be boosted by a significant factor.

Mark Lacy is thanked for helpful discussions. The referee is credited with constructive comments which improved this paper. We are grateful to Sune Toft for calling our attention to an error in our original calculation of the differential reddening. Support for this work was provided by NASA through grant GO-8202 from the Space Telescope Science Institute, which is operated by AURA under NASA contract NAS 5-26555. We also acknowledge support from NSF grant AST 98-02791. This work was performed under the auspices of the Department of Energy by the University of California Lawrence Livermore National Laboratory under contract W-7405-Eng-48. J. N. W. thanks the Fannie and John Hertz Foundation for financial support.

REFERENCES

Boisse, P., Le Brun, V., Bergeron, J., & Deharveng, J.-M. 1998, A&A, 333, 841
Brotherton, M. S., Tran, H. D., Laurent-Muehleisen, S. A., Becker, R. H., White, R. L., & Gregg, M. D. 2000, in preparation
Burstein, D., & Heiles, C. 1982, AJ, 87, 1165
Cardelli, J. A., Clayton, G. C., & Mathis, J. S. 1989, ApJ, 345, 245
Falco, E. E., et al. 1999, ApJ, 523, 617
Filippenko, A. V. 1982, PASP, 94, 715
Fruchter, A. S., & Hook, R. N. 1998 (astro-ph/9808087)
Gardner, J. P., et al. 2000, AJ, 119, 486
Gregg, M. D., Wisotzki, L., Becker, R. H., Schechter, P. L., Maza, J., & White, R. L., 2000, in preparation
Gregg, M. D., & Minniti, D. 1997, PASP, 109, 1062
Holtzman, J. A., et al. 1995, PASP, 107, 156
Jain, D., Panchapakesan, N., Mahajan, S., & Bhatia, V. B. 1999 (astro-ph/9911004)
Kimble, R. A., et al. 1997, ApJ, 492, L83
Kochanek, C., Falco, E. E., Impey, C. D., Lehár, J., McLeod, B. A., Rix, H.-W., Keeton, C. R., Muñoz, J. A., & Peng, C. Y. 2000, in ASP Conf. Ser., Gravitational Lensing: Recent Progress and Future Goals, ed. T. Brainerd & C. Kochanek (San Francisco: ASP), in press
Kochanek, C. S., Falco, E. E., & Muñoz, J. A. 1999b, ApJ, 510, 590
Maoz, D., & Rix, H.-W. 1993, ApJ, 416, 425
Oke, J. B., Cohen, J. G., Carr, M., Cromer, J., Dingizan, A., Harris, F. H., Labrecque, S., Lucinio, R., Schaal, W., Epps, H., & Miller, J. 1995, PASP, 107, 375
Reimers, D., Köhler, T., & Wisotzki, L. 1996, A&AS, 115, 235
Rix, H.-W., et al. 1994, ApJ, 435, 49
Schlegel, D. J., Finkbeiner, D. P., & Davis, M. 1998, ApJ, 500, 525
Turner, E. L., Ostriker, J. P., & Gott, J. R., III. 1984, ApJ, 284, 1
Wambsganss, J., & Paczyński, B. 1991, AJ, 102, 864
White, R. L., et al. 2000, ApJS, 126, 133
Wisotzki, L., Köhler, T., Groote, D., & Reimers, D. 1996, A&AS, 115, 227
Wisotzki, L., Köhler, T., Kayser, R., & Reimers, D. 1993, A&A, 278, L15
Woodgate, B. E., et al. 1998, PASP, 110, 1183